AIP | Applied Physics Letters

Understanding the anisotropic initiation sensitivity of shocked pentaerythritol tetranitrate single crystals

Ki-Hong Kim, Laurence E. Fried, and Jack J. Yoh

Citation: Applied Physics Letters **103**, 131912 (2013); doi: 10.1063/1.4823796
View online: http://dx.doi.org/10.1063/1.4823796
View Table of Contents: http://scitation.aip.org/content/aip/journal/apl/103/13?ver=pdfcov
Published by the AIP Publishing

Understanding the anisotropic initiation sensitivity of shocked pentaerythritol tetranitrate single crystals

Ki-Hong Kim,[1,2] Laurence E. Fried,[2] and Jack J. Yoh[1,a)]
[1]*Department of Mechanical and Aerospace Engineering, Seoul National University, Seoul 151-744, South Korea*
[2]*L-282, Lawrence Livermore National Laboratory, Livermore, California 94550, USA*

(Received 8 August 2013; accepted 13 September 2013; published online 26 September 2013)

Shock initiation experiments of single crystals of pentaerythritol tetranitrate (PETN) have revealed that they show anisotropic sensitivity to mechanical impact. An ignition and growth model is developed based on the empirical observations of these impact studies. Because this model is independent of the direction of compression, the anisotropic material response of single crystals has not been addressed. Here, we present a complete description of the anisotropic ignition and growth of PETN and provide quantitative validations using the experimental data. The model is appropriate for use in single crystal studies of explosive initiation, or in grain scale simulations of composites. © *2013 AIP Publishing LLC*. [http://dx.doi.org/10.1063/1.4823796]

Anisotropic sensitivity has been observed in shock initiation experiments on pentaerythritol tetranitrate (PETN) single crystals.[1–3] The existence of a preferred orientation of crystal slip explains why the pressure threshold for detonating PETN along the ⟨100⟩ direction is at least four times higher than that along the ⟨110⟩ direction.[4,5] Experiments[1–3,5] and molecular simulations[4,6,7] both suggest that coupling between thermal, chemical, and mechanical effects is needed to properly address the anisotropic behavior of PETN.

Table I summarizes the measured input stresses for PETN shock initiation experiments.[1] Both the ⟨110⟩ and ⟨001⟩ directions are shown to be initiable at 8.6 GPa, while the ⟨101⟩ and ⟨100⟩ directions exhibit insensitivity to shock pressures below 19.5 GPa. This physical anomaly was explained by the microscopic concept[2] of a steric hindrance effect. Characteristics of steady detonation, such as the detonation velocity, von Neumann spike, and Chapman-Jouguet (C-J) pressure are independent of crystal orientation.

In a continuum framework, the ignition and growth (I & G) model[8,9] has been widely used to model the shock to detonation transition. Since the model is independent of the direction of compression (isotropic), it is impossible to address the anisotropic shock sensitivity. In this paper, we formulate a complete set of governing equations that incorporate shock initiation data for PETN, and suggest a crystal orientation dependent reactive flow model. A general tensor is used to address three-dimensional effect of the dependence of the strain field on initiation of PETN.

In our reactive flow model, we use a single progress variable λ to describe the degree of reaction. λ varies from 0 (unreacted explosive) to 1 (fully reacted explosive) during the course of the simulation. t is the time, x is the position, p is the pressure, and u is the flow velocity. Given these quantities, we define a direction-dependent shock initiation rate law defined by

$$\frac{\partial \lambda}{\partial t}+\sum_i \frac{\partial \lambda u_i}{\partial x_i}=\begin{cases} I(1-\lambda)^b\left[\sum_{i,j} f\left(\frac{\varepsilon_{ij}}{\varepsilon_{ij,0}}-J_{ij}\right)H(\dot{\varepsilon}_{ij})\right]^X & 0<\lambda<\lambda_{\text{igmax}} \\ +(1-\lambda)^c\lambda^d p^Y\sum_{i,j} G_{1,ij}H(\dot{\varepsilon}_{ij}) & 0<\lambda<\lambda_{\text{G1max}} \\ +G_2(1-\lambda)^e\lambda^g p^Z & \lambda_{\text{G2min}}<\lambda<1, \end{cases} \tag{1}$$

where λ is the reaction progress variable, p is the pressure, ε_{ij} is the strain tensor, and $\dot{\varepsilon}_{ij}$ is the strain rate tensor. $\varepsilon_{ij,0}$ and $\dot{\varepsilon}_{ij,0}$ are reference coefficients, J_{ij} is a unit matrix of all ones, and $H(\dot{\varepsilon}_{ij})$ is a loading function

$$\varepsilon_{ij}=\begin{pmatrix}\varepsilon_{xx} & \varepsilon_{xy} & \varepsilon_{xz}\\ \varepsilon_{yx} & \varepsilon_{yy} & \varepsilon_{yz}\\ \varepsilon_{zx} & \varepsilon_{zy} & \varepsilon_{zz}\end{pmatrix},\quad \dot{\varepsilon}_{ij}=\frac{1}{2}\left(\frac{\partial u_i}{\partial x_j}+\frac{\partial u_j}{\partial x_i}\right),$$

$$H(\dot{\varepsilon}_{ij}(t))=\begin{cases}1 \text{ if } \dot{\varepsilon}_{ij}(t_0)\le\dot{\varepsilon}_{ij,0} \text{ for } i=j, \text{ any } t_0\le t\\ \frac{1}{2} \text{ if } \dot{\varepsilon}_{ij}(t_0)\le\dot{\varepsilon}_{ij,0} \text{ for } i\ne j, \text{ any } t_0\le t\\ 0 \text{ otherwise}\end{cases},$$

The input strength is assumed larger or equal to the base (reference) strain such that

a)Electronic mail: jjyoh@snu.ac.kr. Tel.: 82-2-880-9334.

TABLE I. PETN shock initiation data (see Ref. 1).

Shock direction	Input stress (GPa)	Run distance to detonation (mm)
⟨110⟩	8.6	7.3
⟨110⟩	12.4	4.6
⟨001⟩	12.4	9.5
⟨101⟩	8.6	No go below 19.5 GPa
⟨100⟩	12.4	No go below 19.5 GPa

$$f(\arg) = \begin{cases} \arg & \text{if } \arg > 0 \\ 0 & \text{otherwise} \end{cases}. \tag{2}$$

The first (ignition) term on the right hand side of Eq. (1) is controlled by the strain relative to its reference strain constant in a specific crystal orientation. The function H sets a limiting compressive strain rate required to begin ignition. The second term describes the early growth phase of reaction and is governed by pressure. The third term describes the later stages of reaction and is assumed to be isotropic. The reference strain rates $\dot{\varepsilon}_{ij,0}$ are constants used to control the onset of reaction. Typical values encountered in experiments are tabulated in Table II. The model has been developed to possibly encompass static, ramp, or shock compression, although only shock compression is studied here. The strain and strain rate based terms effectively model the response of hot spots to compression.[8,9]

For strong shocks comparable with the C-J pressure of 31 GPa, the ignition term will trigger rapid reaction along any direction. For weaker shock waves, the anisotropic sensitivity as implemented in the ignition term of Eq. (1) allows the initial pressure to build up along the sensitive direction, which then leads to a full detonation of PETN with the exothermic growth terms of Eq. (1).

The complete governing equations of reactive flow include the conservation of mass, momentum, energy and species, and can be expressed in two-dimensional cylindrical coordinates as follows:

$$\frac{\partial \rho}{\partial t} + \frac{\partial \rho u_r}{\partial r} + \frac{\partial \rho u_z}{\partial z} = 0, \tag{3}$$

$$\frac{\partial \rho u_r}{\partial t} + \frac{\partial (\rho u_r^2 + p)}{\partial r} + \frac{\partial \rho u_r u_z}{\partial z} = 0, \tag{4}$$

$$\frac{\partial \rho u_z}{\partial t} + \frac{\partial \rho u_z u_r}{\partial r} + \frac{\partial (\rho u_z^2 + p)}{\partial z} = 0, \tag{5}$$

$$\frac{\partial \rho E}{\partial t} + \frac{\partial u_r(\rho E + p)}{\partial r} + \frac{\partial u_z(\rho E + p)}{\partial z} = 0, \tag{6}$$

TABLE II. Regime of physical strain rates (see Ref. 10).

Strain rate (1/s)	Impact velocity (m/s)	Effect
$<10^{-5}$	…	Creep
10^{-5}–10^{1}	<50	Primarily elastic
10^{1}–10^{3}	50–500	Primarily plastic
10^{3}–10^{5}	500–1000	Material strength significant
10^{5}–10^{6}	1000–3000	Pressure ~ material strength
10^{6}–10^{8}	3000–12 000	Pressure > material strength
$>10^{8}$	>12 000	Ionization

TABLE III. Parameters for anisotropic rate law.

Parameter	Value
I (1/μs)	100
b, c, e, g	0.667
D	0.01
$\varepsilon_{\langle 001\rangle,0}$, $\varepsilon_{\langle 110\rangle,0}$, $\varepsilon_{\langle 100\rangle,0}$	−0.199
X	8
$G_{1\langle 110\rangle}$ (Mbar^{-Y}/μs)	0.15
$G_{1\langle 001\rangle}$ (Mbar^{-Y}/μs)	0.015
$G_{1\langle 100\rangle}$ (Mbar^{-Y}/μs)	0.001
Y	1
G_2 (Mbar^{-Z}/μs)	1500
Z	2
λ_{igmax}, λ_{G1max}, λ_{G2min}	0.01
$\dot{\varepsilon}_{\langle 110\rangle}$, $\dot{\varepsilon}_{\langle 001\rangle}$ (1/μs)	−1600
$\dot{\varepsilon}_{\langle 100\rangle}$ (1/μs)	−4200

$$\begin{aligned} \frac{\partial \lambda}{\partial t} + \frac{\partial \lambda u_r}{\partial r} + \frac{\partial \lambda u_z}{\partial z} = I(1-\lambda)^b \Bigg[& f\left(\frac{\varepsilon_{rr}}{\varepsilon_{rr,0}} - 1\right) H(\dot{\varepsilon}_{rr}) \\ & + f\left(\frac{\varepsilon_{zz}}{\varepsilon_{zz,0}} - 1\right) H(\dot{\varepsilon}_{zz}) \\ & + f\left(\frac{\varepsilon_{rz}}{\varepsilon_{rz,0}} - 1\right) H(\dot{\varepsilon}_{rz}) \Bigg]^X \\ & + [G_{1,rr} H(\dot{\varepsilon}_{rr}) + G_{1,zz} H(\dot{\varepsilon}_{zz}) \\ & + G_{1,rz} H(\dot{\varepsilon}_{rz})](1-\lambda)^c \lambda^d p^Y \\ & + G_2 (1-\lambda)^e \lambda^g p^Z, \end{aligned} \tag{7}$$

where ρ is density, u_r and u_z are velocity components in radial and axial directions, respectively, E is the total energy per unit mass, and p is the hydrostatic pressure. The switching of the ignition and growth terms is omitted for brevity and is the same as in Eq. (1). We implicitly model molecular-scale dislocation and slip systems through the orientation and strain rate dependence of the ignition and growth terms. We assume that the growth of the explosive

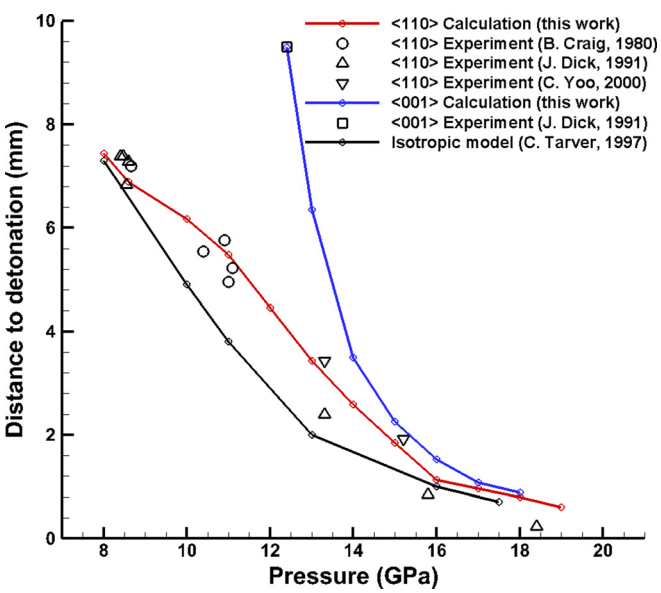

FIG. 1. Dependence of the distance to detonation of PETN on input shock stress in the sensitive orientations of ⟨110⟩ and ⟨001⟩.

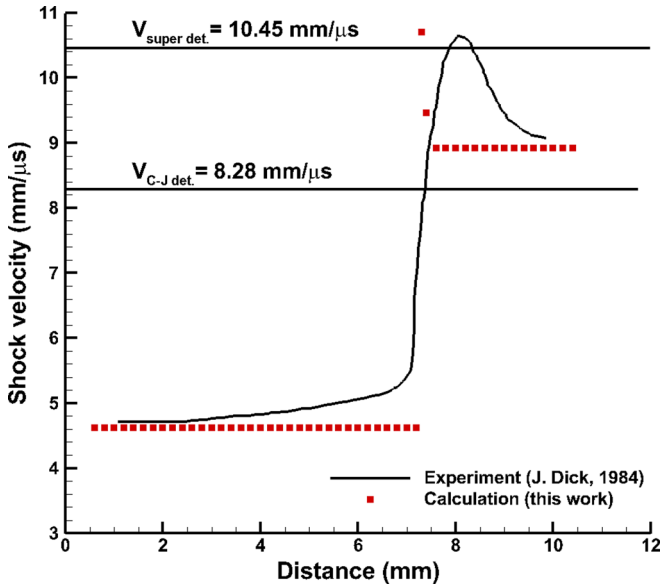

FIG. 2. Dependence of shock velocity on run distance for PETN crystal shocked along the ⟨110⟩ direction at 8.6 GPa. Measured C-J and super detonation velocities shown are from Holland *et al.*[15]

reaction is controlled by shock pressure, and we neglect the elastic-plastic behavior of PETN[13] for the relatively strong shock compressions considered here. The Jones-Wilkins-Lee (JWL) equation of state (EOS) is used to model the high pressure characteristics of both reacted and unreacted PETN, with values given by Tarver *et al.*[9]

$$p = A\left(1 - \frac{\omega}{R_1 V}\right)e^{-R_1 V} + B\left(1 - \frac{\omega}{R_2 V}\right)e^{-R_2 V} + \frac{\omega E}{V}. \quad (8)$$

In this equation, V is the volume relative to its initial value and E is the energy per unit volume. Table III summarizes the anisotropic chemical kinetics parameters used in the simulation.

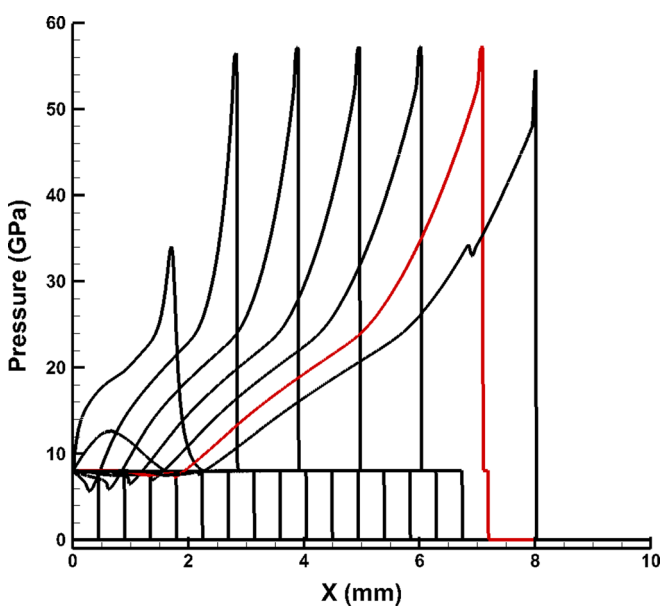

FIG. 3. The calculated pressure evolution is recorded at every 0.1 μs for 8 GPa impact along the sensitive ⟨110⟩ direction. The red line indicates the time at which the unreacted shock wave is overtaken by the reacted shock wave.

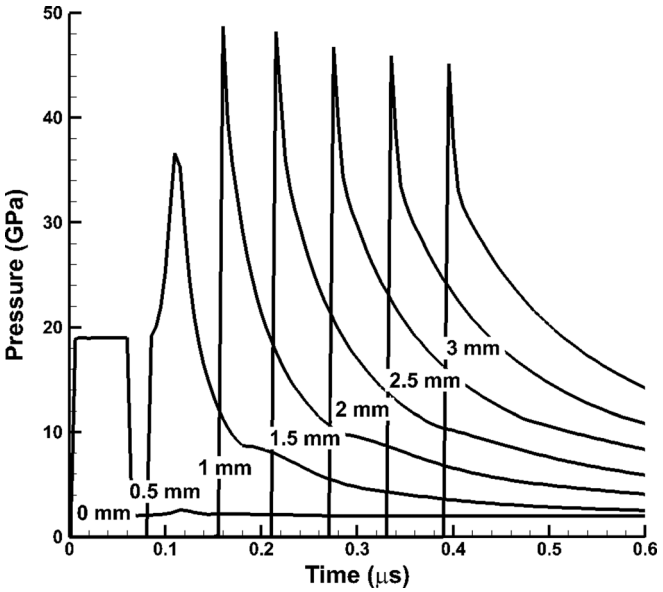

FIG. 4. The calculated pressure history is shown for shock initiation of a translucent PETN pellet by a Mylar flyer plate.

One-dimensional shock compression of PETN is performed. For comparison, both the original I & G (Eq. (9)) and anisotropic rate laws (Eq. (10)) are written out explicitly

$$\frac{\partial \lambda}{\partial t} + \frac{\partial \lambda u}{\partial x} = I(1-\lambda)^b \left(\frac{\rho}{\rho_0} - 1 - a\right)^X + G_1(1-\lambda)^c \lambda^d p^Y + G_2(1-\lambda)^e \lambda^g p^Z, \quad (9)$$

$$\frac{\partial \lambda}{\partial t} + \frac{\partial \lambda u}{\partial x} = I(1-\lambda)^b \left[f\left(\frac{\varepsilon_{xx}}{\varepsilon_{xx,0}} - 1\right) H(\dot{\varepsilon}_{xx})\right]^X + G_{1,xx} H(\dot{\varepsilon}_{xx})(1-\lambda)^c \lambda^d p^Y + G_2(1-\lambda)^e \lambda^g p^Z. \quad (10)$$

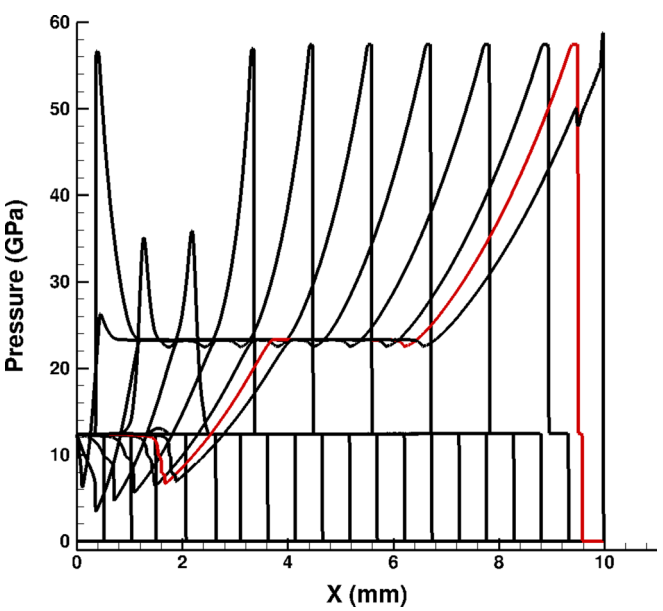

FIG. 5. The calculated pressure evolution is recorded at every 0.1 μs for 12.4 GPa impact on the intermediate sensitivity ⟨001⟩ direction. The red line indicates the time at which the unreacted shock wave is overtaken by the reacted wave.

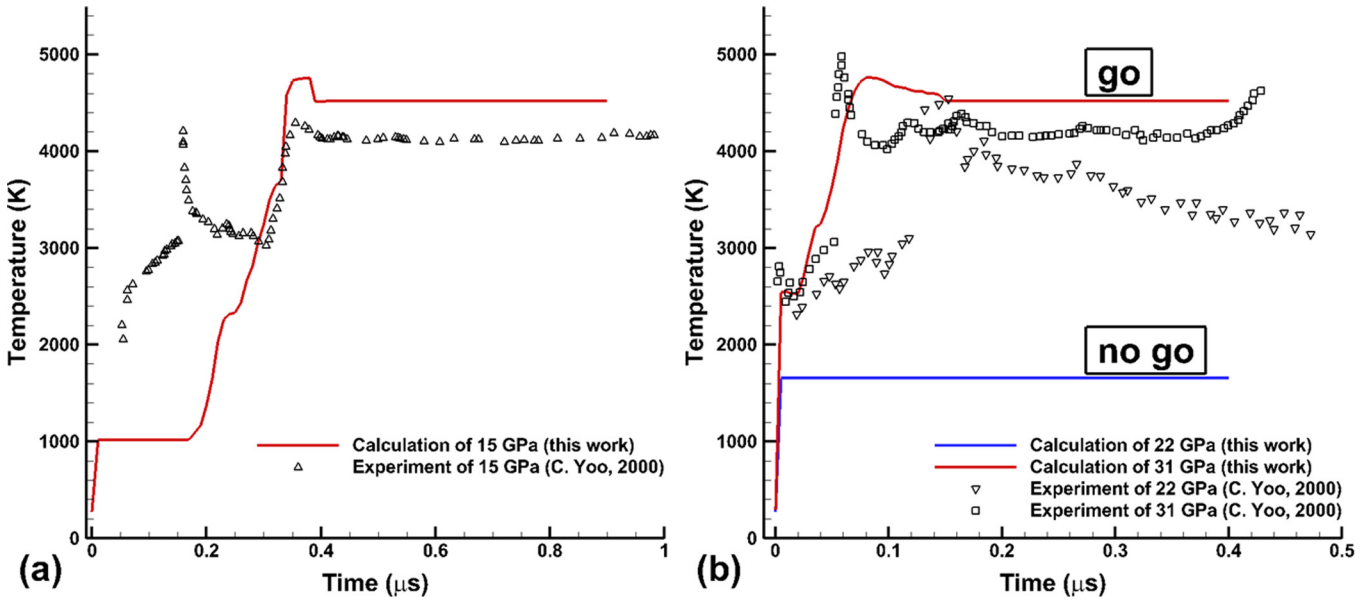

FIG. 6. Time-resolved temperature of PETN single crystals: (a) ⟨110⟩ orientation and (b) ⟨100⟩ orientation.

The isotropic parameters for PETN are from Refs. 8 and 9. A uniform mesh of 2.5 μm/zone is used because of the thin zone reaction length ~40 μm, and the impact pressure varied from 8 to 19 GPa. In the one dimensional approximation studied here, parameters are developed separately for each propagation direction considered, as given by Table III. Figure 1 compares the experimental and calculated run distance to detonation. This quantity is defined as the distance required for the shock wave to be overtaken by the reaction front.[3,8,9,11,12] Our results accurately reproduced the experimental data in the ⟨110⟩ and captured the anticipated ignition behavior in the ⟨001⟩ case.

The model also correctly predicts the existence of a super detonation[1] for pre-compressed PETN that accelerates the reaction rate. In Fig. 2, the pressure and shock velocity in the super detonation regime are significantly higher than their respective C-J values. For an impact pressure of 8 GPa, the time evolution graph in Fig. 3 clearly marks the von Neumann spike (unreacted EOS) pressure of 45 GPa. The C-J pressure of 33 GPa is also in a good agreement with experimental data. We have applied the anisotropic model to an ignition experiment[9] involving initiation by a Mylar flyer. The Mylar flyer plate with velocity close to 4.1 km/s imparts 19 GPa to the PETN during 0.06 μs. The calculated pressure history in Fig. 4 shows well-resolved shock initiation, overdriven super detonation, and pressure decay toward the C-J value. These features are very similar to those calculated with the isotropic I & G model in Ref. 9. Next, the intermediate sensitivity ⟨001⟩ orientation for an impact of 12.4 GPa is considered. The anisotropic model reproduces the time to detonation represented by the red line in Fig. 5 (experiment: 9.4 mm, simulation 9.5 mm), while the isotropic model cannot handle this case.

The time-resolved temperature measured by photomultiplier tubes (PMTs) provides valuable experimental insight into the temporal characteristics of ignition, pressure build-up, and full detonation.[3] The temperature and detonation velocity are measured to be 4140 K and 8.2 mm/μs, respectively. Figure 6 illustrates the calculated temperature of the two different orientations for the given impact pressure. Despite the use of a constant specific heat to fit the C-J state and super detonation state of PETN, the comparison reasonably reproduces the anisotropic behavior of PETN.

To summarize, the anisotropic shock sensitivity of single crystal PETN is predicted by the proposed reactive flow model. The strong direction dependence of shock impact tests is accurately described by the strain tensor field formulation for ignition and growth in a continuum reactive flow framework. The anisotropic model should be applicable to many legacy hydrodynamic codes. Predicting the initiation behavior of composite explosives on the basis of physics-based grain scale continuum models is of growing interest.[14] We anticipate that the present model could be used in the grain-scale modeling of pressed powders, to predict the response of other single-crystal experiments, or to model other anisotropic reactive materials or assemblies.

Kim is supported by the NRF postdoctoral fellowship, and Yoh is supported by NRF-ADD projects contracted through IAAT at SNU. This research was partly funded under the auspices of the U.S. Department of Energy by Lawrence Livermore National Laboratory under Contract No. DE-AC52-07NA27344. The authors are grateful to each grant providing agency.

[1]J. J. Dick, Appl. Phys. Lett. **44**, 859 (1984).
[2]J. J. Dick, J. Appl. Phys. **81**, 601 (1997).
[3]C. S. Yoo, N. C. Holmes, P. C. Souers, C. J. Wu, F. H. Ree, and J. J. Dick, J. Appl. Phys. **88**, 70 (2000).
[4]S. V. Zybin, W. A. Goddard III, P. Xu, A. C. T. van Duin, and A. P. Thompson, Appl. Phys. Lett. **96**, 081918 (2010).
[5]I. Plaskin, C. S. Coffey, R. Mendes, J. Ribeiro, J. Campos, and J. Direito, 13th Symposium (International) on Detonation, ONR 351-07-01, 2006, p. 319.
[6]Y. A. Gruzdkov and Y. M. Gupta, J. Phys. Chem. **104**, 11169 (2000).
[7]P. Maffre and M. Peyrard, Phys. Rev. B **45**, 9551 (1992).
[8]E. L. Lee and C. M. Tarver, Phys. Fluids **23**, 2362 (1980).
[9]C. M. Tarver, R. D. Breithaupt, and J. W. Kury, J. Appl. Phys. **81**, 7193 (1997).

[10]R. F. Bunshah, *Techniques of Metals Research, Measurement of Mechanical Properties* (Wiley, New York, 1971), Vol. 5, p. 244.
[11]K. Kim and J. J. Yoh, Proc. Combust. Inst. **34**, 2025 (2013).
[12]J. J. Dick, R. N. Mulford, W. J. Spencer, D. R. Pettit, E. Garcia, and D. C. Shaw, J. Appl. Phys. **70**, 3572 (1991).
[13]J. M. Winey and Y. M. Gupta, J. Appl. Phys. **107**, 103505 (2010).
[14]R. Menikoff and T. D. Sewell, Combust. Theory Modell. **6**, 103–125 (2002).
[15]T. E. Holland, A. W. Campbell, and M. E. Malin, J. Appl. Phys. **28**, 1217 (1957).